64-C

REPORT NO. RF-TR-63-16

COPY 19

AN ANALYTICAL DETERMINATION OF THE RADAR CROSS SECTION OF CERTAIN MISSILE-LIKE CONFIGURATIONS

13 August 1963

U S ARMY MISSILE COMMAND
REDSTONE ARSENAL, ALABAMA

13 August 1963 Report No. RF-TR-63-16

AN ANALYTICAL DETERMINATION OF THE RADAR CROSS SECTION OF CERTAIN MISSILE-LIKE CONFIGURATIONS

By

Robert J. Chynoweth
Robert R. Boothe

Department of the Army Project No. 1-B-2-22901-A-204
AMC Management Structure Code No. 5221.11.146

Advanced Systems Laboratory
Directorate of Research and Development
U. S. Army Missile Command
Redstone Arsenal, Alabama

ABSTRACT

This report is concerned with the description of the assumptions, methods, and equations used by the Advanced Systems Laboratory, USAMICOM, in the analytical determination of the radar cross section of various missile configurations. The method used is primarily that of physical optics. Examples, using the physical optics integral, are included. Two methods of computing the cross section are given: (1) phase addition--giving a complex pattern and, (2) random addition--giving an effective pattern.

ACKNOWLEDGMENT

The authors wish to thank Messrs. M. Bechel and R. Wohlers of Cornell Aeronautical Laboratories for their helpful comments on the material content of this report.

TABLE OF CONTENTS

LIST OF SYMBOLS

α	=	Lower limit of integration along Z, or cone half-angle as appropriate
α_i	=	Appropriate half-angle of cone or frustum
a_i	=	Appropriate base radius of cone or frustum
A	=	Projected cross-sectional area of body in direction of propagation
β	=	Upper limit of integration along Z
D	=	Distance between scatterers
K	=	Propagation constant
λ	=	Wavelength of radiation
L	=	Axial length of cone
N	=	$\pi \tan^2 \alpha$
ϕ	=	Angle between normal to the body and the direction of propagation
ϕ_i	=	Phase angle difference between scatterers
P	=	i2K
r	=	Projection of radius of curvature in plane normal to the direction of propagation
R or R_i	=	Appropriate radius of curvature
σ	=	Radar cross section
RE	=	Real component of cross section
IM	=	Imaginary component of cross section
S	=	Path of integration along surface of body normal to direction of propagation
θ	=	Aspect angle - angle measured between nose-on and propagation vector
Z	=	Direction of propagation

AN ANALYTICAL DETERMINATION OF THE RADAR CROSS SECTION OF CERTAIN MISSILE-LIKE CONFIGURATIONS

I. INTRODUCTION

There have been many attempts at analytically defining the radar cross section of various missile shapes. The investigations by Dr. K. M. Diegal et al., at the University of Michigan and personnel of Cornell Aeronautical Laboratories, are to be noted. This report was written to supplement the efforts of these investigators.

The need for the radar cross section of certain missile configurations, prompted the authors to study the various techniques used to compute this quantity. It was noted that many formulas existed, but a clear, concise derivation was invariably omitted. (The derivations were needed so that if it became necessary to compute the cross section where there were no analytical expressions, we could derive our own.) It was noted at the start that the method using physical optics gave creditable answers, therefore this method was used throughout. The formulas that result from using this method were programmed on the IBM 7090, for use by this laboratory.

To make this report a workable document, all classified material was deleted. A separate report will be published in the future, showing a comparison between the analytical results and measured data of certain missile configurations. The measurements were made on the scale model ranges of Cornell Aeronautical Laboratories, Buffalo, N. Y., and the full scale facility of the Radio Corporation of America, Moorestown, N. J.

This report is concerned with the description of the assumptions, methods, and equations used by this laboratory in the analytical determination of the radar cross section of various missile configurations.

Scattering of electromagnetic waves is a very complex phenomenon that depends upon such factors as the shape, orientation, and composition of the scattering body, the polarization and frequency of the incident energy, and the angular separation between the transmitter or source of energy, and the receiving device. The angular separation between the radar system elements is commonly known as the "bistatic angle." Only the monostatic condition where the radar transmitter and receiver are at the same site will be discussed here.

As a matter of definition, the cross section for scattering in any specified direction is 4π times the ratio of scattered power per unit solid angle to the incident power per unit area. It is noted therefore that the units for the radar cross section will dimensionally be in area, the accepted units being square meters (m^2). An exact theoretical determination of the radar cross section of a particular configuration is a complex undertaking, especially for those other than the most simple shapes. Such analytical calculation constitute a rigorous solution of Maxwell's equations with application of boundary conditions appropriate to a particular body shape. To date, this has been accomplished for only a small number of simple shapes. Because of time and manpower allocations it has been necessary to resort to the use of approximate methods for the calculation of radar cross section.

II METHOD OF PHYSICAL OPTICS

Of the various approximate methods which are utilized to calculate radar cross section, the method of "physical optics" is most used because of its relative simplicity and valid application to a wide variety of cases. There are certain assumptions, however, that must be recognized in regard to the physical optics theory before application to various missile shapes; these are, the conductivity of the missile radiating surface is assumed to be infinite, the radii of curvature are greater than the wavelength of the incident radiation, and the body is at a sufficiently large distance from the transmitter so that the incident wave is almost nonspherical (planar). A characteristic which is not considered, in this study, is that of the polarization of the incident wave. The cross section results obtained from physical optics are independent of polarization and will therefore differ from experimental results when polarization effects are pronounced. For bodies having scatterers that are independent of polarization such as blunt-nosed missiles, physical optics yields good results.

The basic physical optics equation for the radar cross section in integral form is given in Kerr[1] as:

$$\sigma = \frac{4\pi}{\lambda^2} \left| \int_{\alpha}^{\beta} \frac{dA}{dZ} e^{j2KZ} \, dZ \right|^2 \qquad (1)$$

where

σ = the radar cross section

$\frac{dA}{dZ}$ = the rate of change in the cross sectional area of the body and its shadow in the direction of propagation

Z = the direction of propagation

K = the propagation constant $\left(\frac{2\pi}{\lambda}\right)$

λ = the wavelength of the incident radiation

The physical optics equation (1) is based on the approximation that if a plane wave is incident upon a good conducting surface of convolution having radii of curvature greater than one wavelength, the currents induced on the surface and the fields radiated from any infinitesimal area are approximately equal to those which would be obtained if this small area were part of an infinite plane tangent to the surface of the point of the area considered.

A. Sphere

Equation (1) can be written as $\sqrt{\sigma} = \frac{2\sqrt{\pi}}{\lambda} \int_{\alpha}^{\beta} \frac{dA}{dZ} e^{i2KZ} \, dZ$ (1a.)

where: $K = \frac{2\pi}{\lambda}$

The figure appropriate to this example is

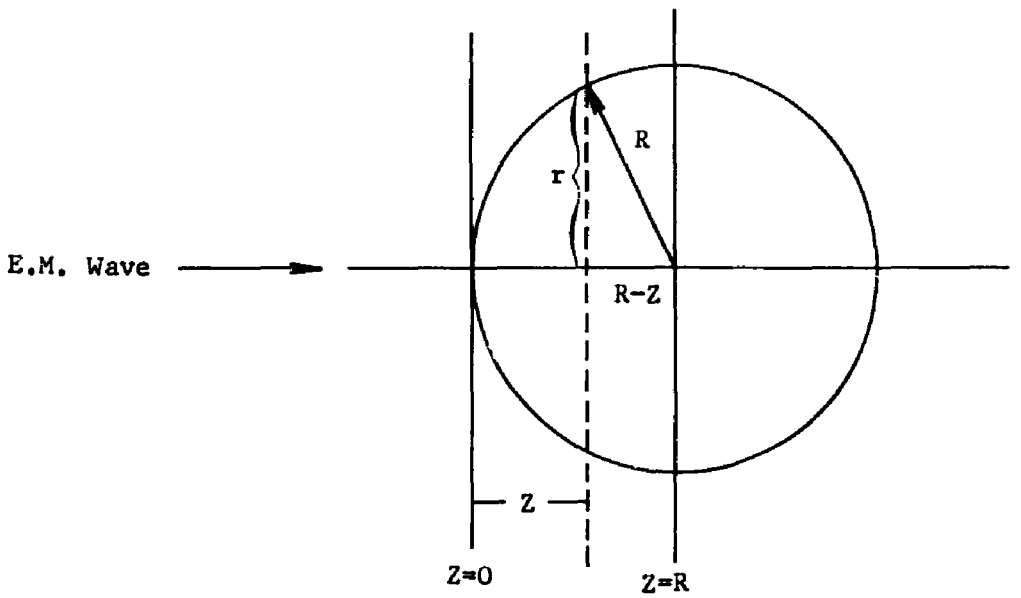

Figure I

The limits of integration will be

$\alpha = 0$

$\beta = R$

From Figure I

$r^2 + (R - Z)2 = R^2$

$r^2 = R^2 - (R - Z)^2$

or

$r^2 = 2RZ - Z^2$

The area of the plane section of the sphere, at Z is $A = \pi r^2$ or

$$A = \pi r^2 = \pi(2RZ - Z^2)$$

therefore

$$\frac{dA}{dZ} = \pi(2R - 2Z)$$

It is now necessary to substitute this value in equation (la

$$\therefore \sqrt{\sigma} = \frac{2\sqrt{\pi}}{\lambda} \int_0^R \left[\pi(2R - 2Z)\right] e^{i2KZ}\, dZ$$

Now separating the integral, we get

$$\sqrt{\sigma} = \frac{4\pi^{2/3}}{\lambda}\left[\int_0^R Re^{i2KZ}\, dZ - \int_0^R Ze^{i2KZ}\, dZ\right]$$

Evaluation of the integrals yields

$$\sqrt{\sigma} = \frac{4\pi^{2/3}}{\lambda}\left\{ R\left[(i2K)^{-1}e^{i2KZ}\right]_0^R - \left[\frac{Z}{i2K}\, e^{i2KZ} - \frac{1}{(i2K)2}\left(e^{i2KZ}\right)\right]_0^R\right\}$$

Substituting the limits and collecting terms

$$\therefore \sqrt{\sigma} = \frac{-4\pi^{3/2}}{\lambda(i2K)^2}\left[R(i2K) - (e^{i2KR} - 1)\right]$$

Since the magnitude of the cross section is to be determined, we can neglect the phase contribution, so that

$$\sqrt{\sigma} = \frac{-4\pi^{3/2}}{\lambda(i2K)^2}\left[R(i2K)\right]$$

Now squaring both sides of the equation and retaining the absolute value

$$\sigma = \pi R^2$$

Therefore, the magnitude of the radar cross section is seen to be equal to the geometrical cross section, as is to be expected. In Appendix I, the radar cross section of a right circular cone is computed using the same procedure as that used on the sphere.

B. Variations of Physical Optics Integral

The integral in equation (1), for certain geometrical shapes, is sometimes very difficult to evaluate. Investigations at Cornell Aeronautical Laboratories[2] have determined the form of the first term of the asymptotic expansion of the physical optics integral for various types of surface configurations. The results which are pertinent to this report are:

1. For surfaces having principal radii of curvature R_1 and R_2 where the inward normal to the surface is in the direction of incident radiation,

$$\sigma = \pi R_1 R_2 \tag{2}$$

2. For curves having a radius of curvature R at the surface where the inward normal to the surface is in the direction of the incident radiation,

$$\sigma = \frac{2\pi}{\lambda} \left| \int_S \sqrt{R}\, dS \right|^2 \tag{3}$$

where the integration is performed along the curve.

3. For curves along slope discontinuities of a surface which lie in a plane which is perpendicular to the incident radiation,

$$\sigma = \frac{1}{4\pi} \left| \int_S \Delta \cot \phi \, dS \right|^2 \tag{4}$$

where $\Delta \cot \phi$ is the change in the cotangent of the angle between the normal to the body and the direction of the incident wave as one crosses the boundary of the curve.

4. For curves that are not in a plane which is perpendicular to the direction of incidence,

$$\sigma = \frac{\lambda}{8\pi} \frac{|\Delta \cot \phi|^3}{\left|\Delta \frac{1}{R}\right|} \qquad (5)$$

where $\Delta \frac{1}{R}$ is the change in curvature of the body across the curve boundary and ϕ is as defined above. The radius of curvature is measured in the plane which is normal to the direction of propagation, and the function is to be evaluated at points where the transition curve is normal to the direction of the incident wave.

It is appropriate at this time to point out some important limitations of physical optics theory. In the application of physical optics to any particular problem, one must keep in mind that the results obtained from the use equations (2) through (5) are based on physical optics theory and are thereby approximate. Therefore, they should be considered valid only when the dimensions of the body are <u>larger</u> than the wavelength. In addition, one should recall that equations (2) through (5) include only the leading term of an asymptotic expansion of equation (1); and on occasion, this approximation can introduce a noticeable error.

Theoretical calculations in the vicinity of nose-on are subject to large errors. Experimental data consistently show a significantly larger return at nose-on than is predicted by physical optics theory. This is attributed to one or a combination of phenomena described by the end-fire, shadow-wave, and nose gain theories. Along the missile longitudinal axis, surface waves in the shadow region as well as the visible surface can combine in phase to produce large returns at nose-on angles.

Equations (2) through (5) can be applied to missile configurations to obtain formulae for the cross section contributions of each predominate scatterer in terms of aspect angle (θ) and body parameters. Equations applicable to the four principle scatterers of Figure II are presented in Appendixes A through D.

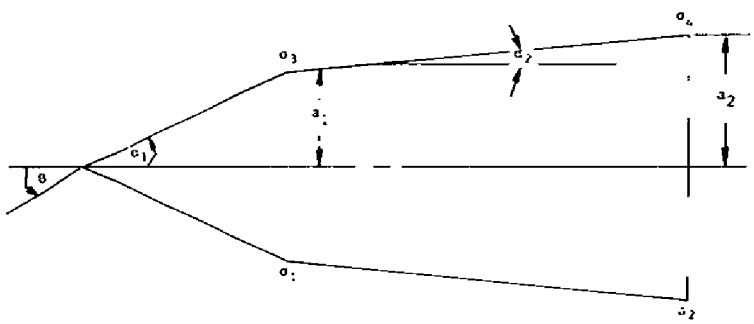

Figure II

C. Cone-Frustum

Utilizing the results of Appendixes A through D, the following equations can be used to calculate the radar cross section contribution of each individual scatterer, at specified aspect angles, for the configuration of Figure II.

Case A (σ_1):

$$\sigma_1 = \frac{\lambda a_1}{8\pi} \frac{(\tan \alpha_1 - \tan \alpha_2)^2}{\sin \theta \cos^4 \theta (1 - \tan \theta \tan \alpha_1)^2 (1 - \tan \theta \tan \alpha_2)^2}$$

for:

$$0 < \theta < \frac{\pi}{2} - \alpha_1 \qquad \frac{\pi}{2} - \alpha_2 < \theta < \frac{\pi}{2}$$

$$\frac{\pi}{2} - \alpha_1 < \theta < \frac{\pi}{2} - \alpha_2 \qquad \frac{\pi}{2} < \theta < \pi - \alpha_1$$

$$\sigma_1 = \frac{\lambda a_1}{8\pi} \frac{\tan^2 (\theta + \alpha_2)}{\sin \theta}$$

for:

$$\pi - \alpha_1 < \theta < \pi - \alpha_2$$

$$\sigma_1 = \frac{\lambda a_1}{8\pi} \frac{(\tan \alpha_1 - \tan \alpha_2)^2}{\tan^2 \alpha_2 \tan^2 \alpha_1}$$

for:

$$\theta = \frac{\pi}{2}$$

$$\sigma_1 = 0$$

for:

$$\pi - \alpha_2 \leq \theta \leq \pi$$

Case B (σ_2):

$$\sigma_2 = \frac{\lambda a_2}{8\pi} \frac{\tan^2 (\theta + \alpha_2)}{\sin \theta}$$

for:

$$0 < \theta < \frac{\pi}{2} - \alpha_2$$

$$\frac{\pi}{2} - \alpha_2 < \theta \leq \frac{\pi}{2}$$

$$\sigma_2 = \frac{\lambda a_2}{8\pi} \frac{1}{\sin^3 \theta \, (\tan \alpha_2 \sin \theta - \cos \theta)^2}$$

for:

$$\frac{\pi}{2} < \theta \leq \pi - \alpha_2$$

$$\sigma_2 = \frac{\lambda a_2}{8\pi} \frac{\cos^2 \theta}{\sin^3 \theta}$$

for:

$$\pi - \alpha_2 < \theta < \pi$$

Case C (σ_3):

$$\sigma_3 = \frac{\lambda a_1}{8\pi} \frac{(\tan \alpha_1 - \tan \alpha_2)^2}{\sin \theta \cos^4 \theta \, (1 + \tan \theta \tan \alpha_1)^2 \, (1 + \tan \theta \tan \alpha_2)^2}$$

for:

$$0 < \theta < \alpha_2$$

$$\sigma_3 = \frac{\lambda a_1}{8\pi} \frac{\tan^2 (\alpha_1 - \theta)}{\sin \theta}$$

for:

$$\alpha_1 \leq \theta \leq \alpha_2$$

$$\sigma_3 = 0$$

for:

$$\alpha_1 \leq \theta \leq \pi$$

Case D (4):

$$\sigma_4 = \frac{\lambda a_2}{8\pi} \frac{\tan^2 (\alpha_2 - \theta)}{\sin \theta}$$

for:

$$0 < \theta \leq \alpha_2$$

$$\sigma_4 = \frac{\lambda a_2}{8\pi} \frac{\cos^2 \theta}{\sin^3 \theta}$$

for:

$$\frac{\pi}{2} < \theta < \pi$$

$$\sigma_4 = 0$$

for:

$$\alpha \leq \theta \leq \frac{\pi}{2}$$

It can be seen, from the proceeding collection of equations, that they become indeterminate whenever the aspect angle becomes equal to $\left(\frac{\pi}{2} - \alpha_1\right)$ or broadside to the cone. To circumvent this condition, it was necessary to compute a separate function for this special case. The application of equation (3) yields

$$\sigma_{side} = \frac{8}{9} \frac{\pi a_1^3}{\lambda \cos \alpha_1 \sin^2 \alpha_1}$$

when

$$\theta = \frac{\pi}{2} - \alpha_1$$

For normal incidence on the side of the frustum, application of equation (3) yields

$$\sigma_{side} = \frac{8}{9} \frac{\pi (a_2^{3/2} - a_1^{3/2})^2}{\lambda \cos \alpha_2 \sin^2 \alpha_2}$$

when

$$\theta = \frac{\pi}{2} - \alpha_2$$

For nose-on incidence ($\theta = 0^\circ$), application of equation (4) to the cone-frustum intersection yields

$$\sigma_{ring\ 1,3} = \pi a_1^2 (\tan \alpha_2 - \tan \alpha_1)^2$$

when

$$\theta = 0^\circ$$

and for the frustum base:

$$\sigma_{\text{ring 2, 4}} = \pi a_2^2 \tan^2 \alpha_2$$

when:

$$\theta = 0^\circ$$

(A derivation of this equation, using equation (1) can be found in Appendix E.)

The scattering from the tip has been neglected in the ASL computer programs because of the extremely small return predicted by physical optics. The equation applicable to the cross section contribution from the tip is

$$\sigma = \frac{\lambda^2 \tan \alpha}{16} \qquad \theta = 0^\circ$$

It can be seen that $\lambda = 0.54$ m (f = 5500 Mc) and it is assumed that the cone half angle (α) is approximately 10°, the radar cross section return is $\approx 10^{-8}$ m^2. This value when added to the returns from the other scatterers is considered negligible.

If the nose is blunted, then at $\theta = 0^\circ$, the return will be:

$$\sigma = \pi R^2 \qquad (R = \text{radius of nose})$$

III. MECHANIZATION OF EQUATIONS

The Advanced Systems Laboratory (ASL) has programmed on the IBM 7090, a method of computing the radar cross section of certain geometrical shapes utilizing the physical optics approximations. Different missile configurations can be evaluated and these are:

A. Cone-Cylinder-Frustum

B. Cone-Frustum

C. Cone-Cylinder

D. Cone

To illustrate the procedure that is used in the computer, the cone-frustum shape is chosen. The cross section equations are found in Appendixes A through D.

A. Complex Cross Section

When the contribution from the individual scatterers have been computed, with the proper aspect angle boundary conditions, they must be combined with the proper phase relationships to obtain the total return as a function of the indicated aspect angle. From, the studies performed at the University of Michigan[3], it can be shown that the total cross section return can be given by

$$\sigma_{total} = \left| \sum_{i=1}^{n} \sqrt{\sigma_i}\, e^{j\phi_i} \right|^2 \qquad (6)$$

where the phase angle difference between the individual return scatterer is given as

$$\phi_i = 2K\, D_{1i} = 2\,\frac{(2\pi)}{\lambda}\, D_{1i}$$

since $\sigma \propto \bar{E}^2$

The phase angle (ϕ_i) can be obtained by passing cutting planes, perpendicular to incoming EM wave, through the individual scattering points. The parallel planes are referenced to the plane passing through the front end of the nose cone. The distance from the reference plane to the individual end of the nose cone. The distance from the reference plane to the individual cutting planes can be established from the geometry of ure III.

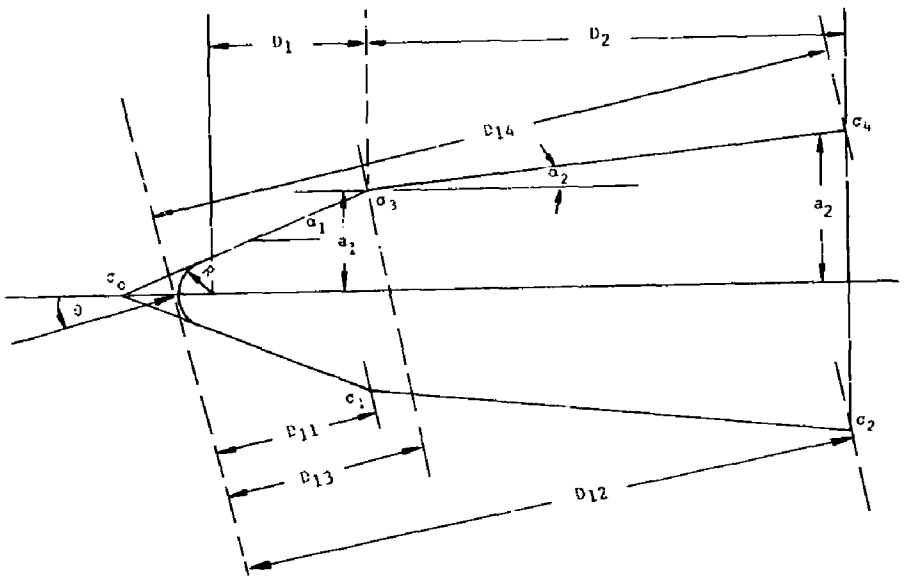

Figure III

From Figure III:

$$D_{11} = R + D_1 \cos\theta - a_1 \sin\theta \tag{7}$$

$$D_{12} = D_{11} + \frac{D_2 \cos(\alpha_2 + \theta)}{\cos\alpha_2} \tag{8}$$

$$D_{13} = D_{11} + 2\, a_1 \sin\theta \tag{9}$$

$$D_{14} = D_{12} + 2\, a_2 \sin\theta \tag{10}$$

(It should be noted that the reference plane is established at the blunted nose radius. If it is desired to compute the cross section of a pointed body then (R) can be set equal to zero, and all formulas remain valid.)

Equations (7) through (10) can be substituted into equation (6) to yield

$$\sqrt{\sigma_{Re}} = \sqrt{\sigma_0} + \sqrt{\sigma_1}\cos\left(\frac{4\pi}{\lambda} D_{11}\right) + \sqrt{\sigma_2}\cos\left(\frac{4\pi}{\lambda} D_{12}\right) + \sqrt{\sigma_3}\cos\left(\frac{4\pi}{\lambda} D_{13}\right) + \sqrt{\sigma_4}\cos\left(\frac{4\pi}{\lambda} D_{14}\right)$$

$$\sqrt{\sigma_{IM}} = \sqrt{\sigma_1}\sin\left(\frac{4\pi}{\lambda} D_{11}\right) + \sqrt{\sigma_2}\sin\left(\frac{4\pi}{\lambda} D_{12}\right) + \sqrt{\sigma_3}\sin\left(\frac{4\pi}{\lambda} D_{13}\right) + \sqrt{\sigma_4}\sin\left(\frac{4\pi}{\lambda} D_{14}\right)$$

It can be shown that

$$\sigma_{total} = \left|\sqrt{\sigma_{Re}} + j\sqrt{\sigma_{IM}}\right|^2$$

and

$$\sigma_T = \left(\sqrt{\sigma_{Re}}\right)^2 + \left(\sqrt{\sigma_{IM}}\right)^2 \tag{11}$$

For $\theta = 0^o$

$$\sigma_{RE_o} = \sqrt{\sigma FR} + \sqrt{\sigma RR} \cos\left(\frac{4\pi}{\lambda} D_2\right)$$

$$\sigma_{IM_o} = \sqrt{\sigma RR} \sin\left(\frac{4\pi}{\lambda} D_2\right)$$

where: FR = Front ring, at cone-frustum junction

RR = Rear ring, at rear of frustum

Then:

$$\sigma_{T_o} = \left(\sqrt{\sigma RE_o}\right)^2 + \left(\sqrt{\sigma IM_o}\right)^2 \tag{12}$$

B. Effective Cross Section

The preceding discussion showed in detail the method used to obtain the complex space-phase radar cross section. A similar technique can be used to find the "effective" cross section. (Effective here means a smoothed curve, i.e., it is assumed that the scatterers are added without regard to phase, random phasing.) To determine the effective pattern, the following relationship is used.

$$\sigma_E = \left|\sum_{i=1}^{n} \sqrt{\sigma_i}\right|^2 \tag{13}$$

therefore

$$\sigma_E = \sum_{i=1}^{n} \sigma_i$$

The equations needed to compute the cross section of the cone-cylinder-frustum, cone-cylinder, and cone configurations are summarized in Appendixes F, G, and H, respectively. These equations can be used with the phase addition procedures outlined above to obtain the total cross section return.

APPENDIX A - CALCULATION OF σ_1

This appendix deals with the application of equation (5) to the near corner of the cone-frustum intersection, i.e., the calculation of σ_1.

Equation (5) is repeated here for reference

$$\sigma = \frac{\lambda}{8\pi} \frac{\left| \Delta \cot \phi \right|^3}{\left| \Delta \frac{1}{R} \right|} \qquad \text{(A-1)}$$

Figure A-I shows the geometry for this derivation.

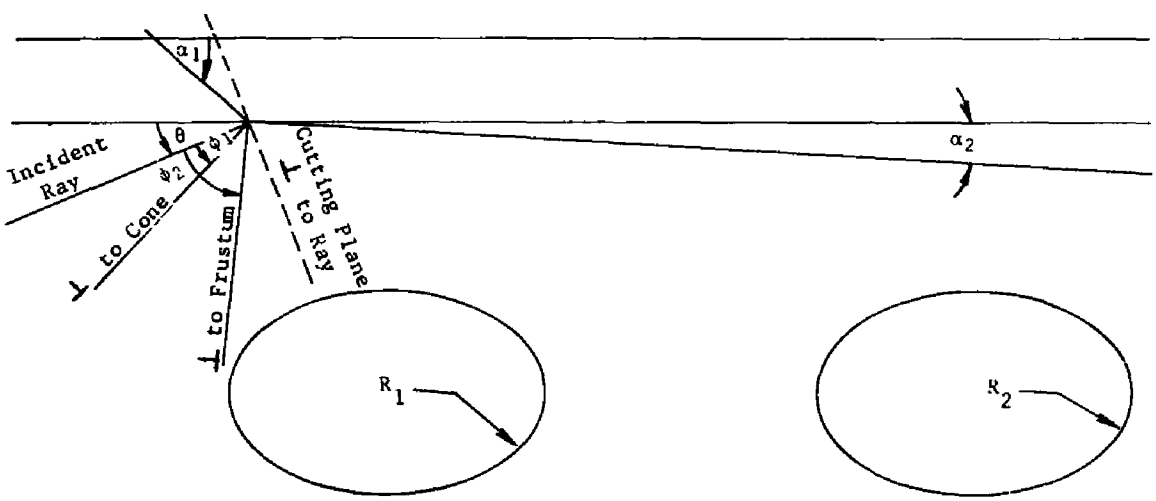

Figure A-I

From this figure:

$$\cot \phi_1 = \cot\left[90^\circ - (\theta + \alpha_1)\right] \qquad \text{(A-2)}$$

or

$$\cot \phi_1 = \tan (\theta + \alpha_1)$$

and

$$\cot \phi_2 = \cot\left[90^\circ - (\theta + \alpha_2)\right]$$

$$\cot \phi_2 = \tan (\theta + \alpha_2) \qquad \text{(A-3)}$$

then

$$|\Delta \cot \phi|^3 = |\cot \phi_1 - \cot \phi_2|^3 \tag{A-4}$$

$$|\Delta \cot \phi|^3 = |\tan (\theta + \alpha_1) - \tan (\theta + \alpha_2)|^3$$

The radii of curvature of the two ellipses obtained by passing a cutting plane through the cone and frustum at the point under consideration are given by:

$$R_1 = a_1 \cos \theta (1 - \tan \theta \tan \alpha_1) \tag{A-5}$$

$$R_2 = a_1 \cos \theta (1 - \tan \theta \tan \alpha_2) \tag{A-6}$$

Then, from (A-5) and (A-6):

$$\left|\Delta \frac{1}{R}\right| = \left|\frac{1}{R_1} - \frac{1}{R_2}\right| \tag{A-7}$$

$$= \left|\frac{1}{a_1 \cos \theta}\left(\frac{1}{1 - \tan \theta \tan \alpha_1} - \frac{1}{1 - \tan \theta \tan \alpha_2}\right)\right|$$

Substituting (A-4), (A-7) into (A-1) yields:

$$\sigma_1 = \frac{\lambda a_1 \cos \theta}{8\pi} \frac{|\tan (\theta + \alpha_1) - \tan (\theta + \alpha_2)|^3}{\left|\frac{1}{1 - \tan \theta \tan \alpha_1} - \frac{1}{1 - \tan \theta \tan \alpha_2}\right|}$$

which reduces to:

$$\sigma_1 = \frac{\lambda a_1 (\tan \alpha_1 - \tan \alpha_2)^2}{8\pi \sin \theta \cos^4 \theta (1 - \tan \theta \tan \alpha_1)^2 (1 - \tan \theta \tan \alpha_2)^2} \tag{A-8}$$

This equation is valid in the region

$$0 < \theta < \frac{\pi}{2} - \alpha_1$$

APPENDIX B - CALCULATION OF σ_2

Application of equation (5) to the near corner of the cone base gives σ_2. Figure B-I shows the geometry for this case.

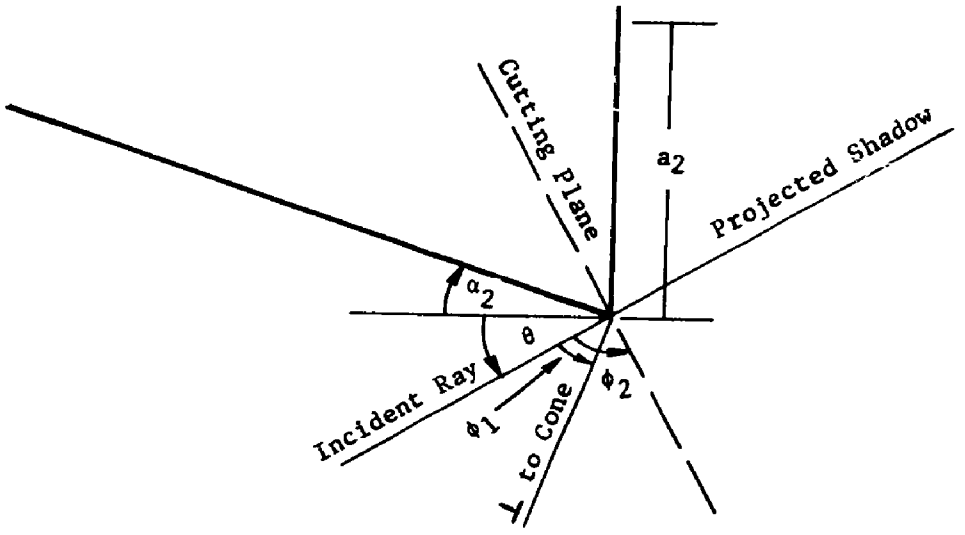

Figure B-I

From this figure:

$$\cot \phi_1 = \cot \left[90^\circ - (\theta + \alpha_2)\right]$$

$$\cot \phi_1 = \tan (\theta + \alpha_2) \qquad \text{(B-1)}$$

and

$$\cot \phi_2 = \cot 90^\circ \qquad \text{(B-2)}$$

$$\cot \phi_2 = 0$$

Then:

$$\left|\Delta \cot \phi\right|^3 = \left|\cot \phi_1 - \cot \phi_2\right|^3$$

$$\left|\Delta \cot \phi\right|^3 = \left|\tan^3 (\theta + \alpha_2)\right| \qquad \text{(B-3)}$$

At the base corner the radii of curvature of the two elliptical segments obtained by passing a cutting plane, first through the cone and then through its projection in the direction of incidence are given by

$$R_1 = a_2 \cos\theta \, (1 - \tan\theta \tan\alpha_2)$$

which reduces to

$$R_1 = \frac{a_2 \cos(\theta + \alpha_2)}{\cos\alpha_2} \tag{B-4}$$

and

$$R_2 = \frac{a_2}{\cos\theta} \tag{B-5}$$

Then, from (B-4) and (B-5)

$$\left|\Delta \frac{1}{R}\right| = \left|\frac{1}{R_1} - \frac{1}{R_2}\right| = \frac{\sin\theta}{a_2} \tan(\theta + \alpha_2) \tag{B-6}$$

Substituting (B-3) and (B-6) into equation (5) yields:

$$\sigma_2 = \frac{\lambda a_2}{8\pi} \frac{\left|\tan^3(\theta + \alpha_2)\right|}{\left|\sin\theta \tan(\theta + \alpha_2)\right|}$$

which reduces to:

$$\sigma_2 = \frac{\lambda a_2}{8\pi} \frac{\tan^2(\theta + \alpha_2)}{\sin\theta} \tag{B-7}$$

This equation is valid in the region

$$0 < \theta < \frac{\pi}{2} - \alpha_2$$

APPENDIX C - CALCULATION OF σ_3

Application of equation (5) to the far corner of the cone-frustum intersection gives σ_3.

Figure C-I shows the geometry for this case.

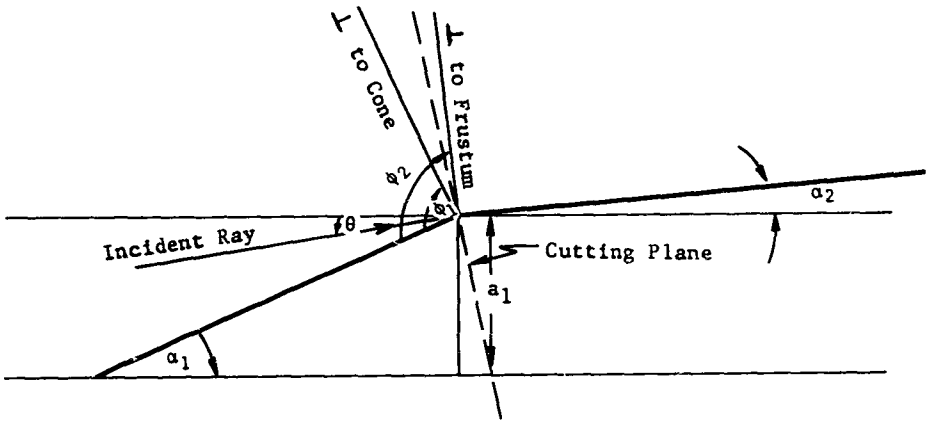

Figure C-I

From this figure:

$$\cot \phi_1 = \cot \left[90^\circ - (\alpha_1 - \theta)\right]$$
$$\therefore \cot \phi_1 = \tan (\alpha_1 - \theta) \qquad \text{(C-1)}$$

and

$$\cot \phi_2 = \cot \left[90^\circ - (\alpha_2 - \theta)\right]$$
$$\therefore \cot \phi_2 = \tan (\alpha_2 - \theta) \qquad \text{(C-2)}$$

Then:

$$\left|\Delta \cot \phi\right|^3 = \left|\cot \phi_1 - \cot \theta_2\right|^3$$
$$\therefore \left|\cot \phi\right|^3 = \left|\tan (\alpha_1 - \theta) - \tan (\alpha_2 - \theta)\right|^3 \qquad \text{(C-3)}$$

The radii of curvature of the two ellipses obtained by passing a cutting plane through the cone and the frustum at the point under consideration are given by:

$$R_1 = a_1 \cos\theta \, (1 + \tan\theta \tan\alpha_1) \tag{C-4}$$

$$R_2 = a_1 \cos\theta \, (1 + \tan\theta \tan\alpha_2) \tag{C-5}$$

Then, from (C-4) and (C-5)

$$\left|\Delta \frac{1}{R}\right| = \left|\frac{1}{R_1} - \frac{1}{R_2}\right| \tag{C-6}$$

$$\therefore \left|\Delta \frac{1}{R}\right| = \left|\frac{1}{a_1 \cos\theta} \left(\frac{1}{1 + \tan\theta \tan\alpha_1} - \frac{1}{1 + \tan\theta \tan\alpha_2}\right)\right|$$

Substituting (C-3) and (C-6) into equation (5) yields:

$$\sigma = \frac{\lambda a_1 \cos\theta}{8\pi} \frac{\left|\tan(\alpha_1 - \theta) - \tan(\alpha_2 - \theta)\right|^3}{\left|\frac{1}{1 + \tan\theta \tan\alpha_1} - \frac{1}{1 + \tan\theta \tan\alpha_2}\right|}$$

which reduces to:

$$\sigma = \frac{\lambda a_1 (\tan\alpha_1 - \tan\alpha_2)^2}{8\pi \sin\theta \cos^4\theta \, (1 + \tan\theta \tan\alpha_1)^2 \, (1 + \tan\theta \tan\alpha_2)^2} \tag{C-7}$$

APPENDIX D - CALCULATION OF σ_4

Application of equation (5) to the far corner of the cone base gives σ_4.

Figure D-I shows the geometry for this case.

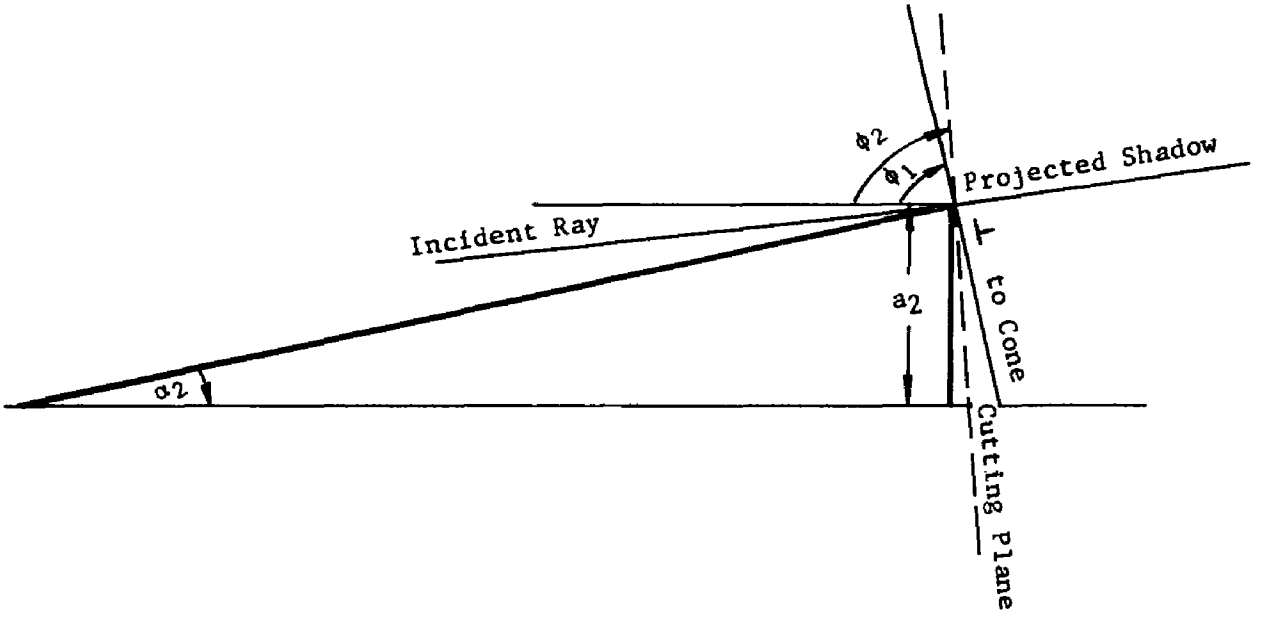

Figure D-I

From this figure:

$$\cot \phi_1 = \cot \left| 90^\circ - (\alpha_2 - \theta) \right|$$

$$\cot \phi_1 = \tan (\alpha_2 - \theta)$$

and

$$\cot \phi_2 = \cot 90^\circ$$

$$\cot \phi_2 = 0$$

Then

$$\left| \Delta \cot \phi \right|^3 = \left| \cot \phi_1 - \cot \phi_2 \right|^3 \qquad (D\text{-}1)$$

$$\left| \Delta \cot \phi \right|^3 = \left| \tan (\alpha_2 - \theta) \right|^3$$

At the base corner, the radii of curvature of the two elliptical segments obtained by passing a cutting plane first through the cone and then through its projected shadow in the direction of incidence are given by

$$R_1 = a_2 \cos\theta \, (1 + \tan\theta \tan\alpha_2)$$

which reduces to

$$R_1 = \frac{a_2 \cos(\alpha_2 - \theta)}{\cos\alpha_2} \tag{D-2}$$

and

$$R_2 = \frac{a_2}{\cos\theta} \tag{D-3}$$

Then, from (D-2) and (D-3)

$$\left|\Delta \frac{1}{R}\right| = \left|\frac{1}{R_1} - \frac{1}{R_2}\right| \tag{D-4}$$

$$\therefore \left|\Delta \frac{1}{R}\right| = \left|\frac{\sin\theta}{a_2} \tan(\alpha_2 - \theta)\right|$$

Substituting (D-1) and (D-4) into equation (5) yields

$$\sigma = \frac{\lambda a_2}{8\pi} \frac{|\tan^3(\alpha_2 - \theta)|}{|\sin\theta \tan(\alpha_2 - \theta)|}$$

which reduces to

$$\sigma_4 = \frac{\lambda a_2}{8\pi} \frac{\tan^2(\alpha_2 - \theta)}{\sin\theta} \tag{D-5}$$

This equation is valid in the region

$$0 < \theta \leq \alpha_2$$

APPENDIX E - CROSS SECTION OF CONE AT NOSE-ON

The radar cross section of a right circular cone at 0° aspect angle (nose-on) will be computed using the basic physical optics integral (Equation 1). Equation (1) is repeated for reference

$$\sqrt{\sigma} = \frac{2\sqrt{\pi}}{\lambda} \int_{\alpha}^{\beta} \frac{dA}{dZ} e^{i2KZ} \, dZ \tag{1}$$

Figure E-1 shows the geometry for this case.

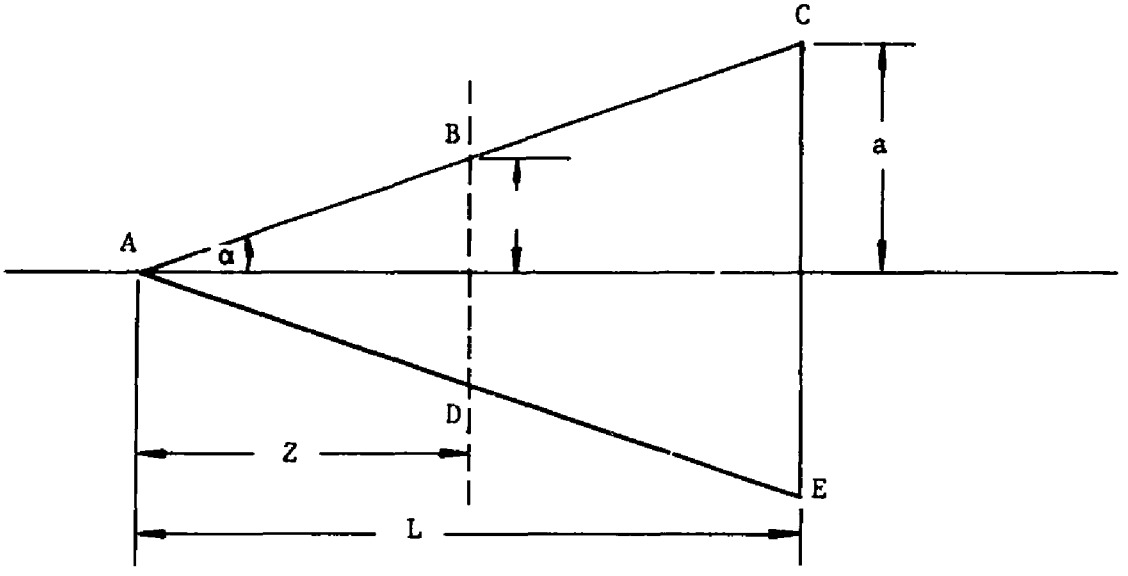

Figure E-1

It is necessary to find the area of the circular section $\overline{BD}$, this can be accomplished as follows:

$$\overline{BD} = A = \pi r^2$$

$$r = Z \tan \alpha$$

therefore

$$A = \pi r^2 = \pi (Z \tan \alpha)^2 \tag{2}$$

$$A = \pi Z^2 \tan^2 \alpha$$

and

$$\frac{dA}{dZ} = 2\pi Z \tan^2 \alpha$$

$$= 2NZ \quad (N = \pi \tan^2 \alpha)$$

Substituting this value into equation (1)

$$\sqrt{\sigma} = \frac{2\sqrt{\pi}}{\lambda} \int_0^L (2NZ)\, e^{i2KZ}\, dZ$$

where the limits of integration are determined by the value of Z (Z=0 at the cone tip).

Now:

$$\sqrt{\sigma} = \frac{4N\sqrt{\pi}}{\lambda} \int_0^L Z\, e^{i2KZ}\, dZ$$

$$= \frac{4N\sqrt{\pi}}{\lambda} \left[\frac{e^{i2KL}}{(i2K)^2} (i2KL - 1) + \frac{1}{(i2K)^2} \right]$$

This equation can be written as:

$$\sqrt{\sigma} = \frac{4N\sqrt{\pi}}{\lambda} \underbrace{\left[\frac{e^{i2KL}}{(i2K)^2} (i2KL - 1) \right]}_{A} + \underbrace{\frac{4N\sqrt{\pi}}{\lambda} \left[\frac{1}{(i2K)^2} \right]}_{B} \qquad (3)$$

A = contribution from the back ring.

B = contribution from the tip.

Thus $\sqrt{\sigma} = A + B$

To solve for the contribution from the back ring, let

$$\sqrt{\sigma} = \frac{4N\sqrt{\pi}}{\lambda} \left[\frac{e^{PL}}{P2} (PL - 1) \right]$$

where

$$P = i2K, \quad K = \frac{2\pi}{\lambda}$$

Now

$$|\sigma| = \left| \frac{16N^2\pi}{\lambda} \left[\frac{e^{2PL}}{P^4} (P^2L^2 - 2PL + 1) \right] \right| \qquad (4)$$

It can be seen that

$$P = i2K = \frac{4i\pi}{\lambda}$$

$$P^2 = \frac{-16\pi^2}{\lambda^2}$$

$$P^3 = \frac{-64i\pi^3}{\lambda^3}$$

$$P4 = \frac{256\pi^4}{\lambda^4}$$

From complex number analysis

$$e^{ni\theta} = \cos n\theta + i \sin n\theta$$

$$\therefore \left| e^{2PL} \right| = \left| \cos \left(\frac{4L}{\lambda}\right)(2\pi) + i \sin \left(\frac{4L}{\lambda}\right)(2\pi) \right|$$

or

$$\left| e^{2PL} \right| = 1$$

Substituting the values for P, P^2, ... and e^{2PL} into equation (4), then

$$|\sigma| = \frac{16N^2\pi}{\lambda^2} \left[\frac{L^2}{P^2} - \frac{2L}{P^3} + \frac{1}{P^4} \right]$$

The terms involving P^3 and P^4 will produce a negligible contribution, therefore neglecting these terms and substituting the value of (N),

$$|\sigma| = \frac{16\pi^3 \tan^4 \alpha}{\lambda^2} \left[\frac{\lambda^2 L^2}{16\pi^2} \right]$$

or

$$|\sigma| = \pi L^2 \tan^4 \alpha \qquad (5)$$

To solve for the contribution from the tip,

$$\sqrt{\sigma} = \frac{4N\sqrt{\pi}}{\lambda} \frac{1}{(i2K)^2}$$

$$\therefore |\sigma| = \frac{\lambda^2 \tan^4 \alpha}{16\pi} \qquad (6)$$

APPENDIX F - CROSS SECTION OF CONE-CYLINDER-FRUSTUM

The radar cross section equations pertaining to the cone-cylinder-frustum configuration are given here, without any attempt at showing derivation. (The equations were derived using the techniques outlined in the test.) Figure F-1 shows the geometry for this case.

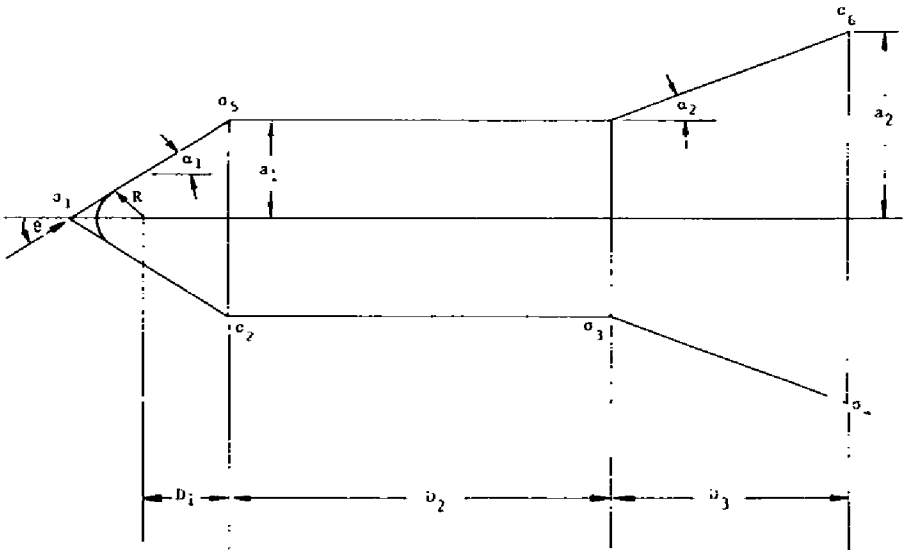

Figure F-1

$$\sigma_1 = \pi R^2 \text{ (If nose is blunted)}$$

$$\sigma_2 = \frac{\lambda a_1}{8\pi} \frac{\tan^2 \alpha_1}{\sin \theta \cos^4 \theta (1 - \tan \theta \tan \alpha_1)^2}$$

$$\sigma_3 = \frac{\lambda a_1}{8\pi} \frac{\tan^2 \alpha_2}{\sin \theta \cos^4 \theta (1 - \tan \theta \tan \alpha_2)^2}$$

$$\sigma_4 = \frac{\lambda a_2}{8\pi} \frac{\tan^2 (\theta + \alpha_2)}{\sin \theta}$$

$$\sigma_5 = \frac{\lambda a_2}{8\pi} \frac{\tan^2 (\alpha_1 - \theta)}{\sin \theta}$$

$$\sigma_6 = \frac{\lambda a_2}{8\pi} \frac{\tan^2 (\alpha_2 - \theta)}{\sin \theta}$$

For normal incidence on the side of the front cone,

$$\sigma_{\text{side 1}} = \frac{8}{9} \frac{\pi a_1^3}{\lambda \cos \alpha_1 \sin^2 \alpha 1} \qquad \theta = \frac{\pi}{2} - \alpha_1$$

For normal incidence on the side of the frustum cone,

$$\sigma_{\text{side 2}} = \frac{8}{9} \frac{\pi \left(a_2 3/2 - a_1 3/2\right)^2}{\lambda \cos \alpha_2 \sin^2 \alpha_2} \qquad \theta = \frac{\pi}{2} - \alpha_2$$

For nose-on incidence ($\theta = 0°$)

$$\sigma_{\text{ring 2,5}} = \pi a_1^2 (\tan \alpha_2 - \tan \alpha_1)^2$$

$$\sigma_{\text{ring 4,6}} = \pi a_2^2 \tan^2 \alpha_2$$

The geometrical distances of the cutting planes from the front reference plane (see text) are:

$$D_{12} = R + D_1 \cos \theta - a_1 \sin \theta$$

$$D_{13} = D_{12} + D_2 \cos \theta$$

$$D_{14} = D_{13} + \frac{D_3 \cos (\alpha_2 + \theta)}{\cos \alpha_2}$$

$$D_{15} = D_{12} + 2a_1 \sin \theta$$

$$D_{16} = D_{14} + 2a_2 \sin \theta$$

APPENDIX G - CROSS SECTION OF CONE-CYLINDER

This appendix describes the equations used to compute the cross section returns for the individual scatterers of the cone-cylinder configuration. The configuration considered is shown in Figure G-1. (These equations are valid for $\theta < \frac{\pi}{2}$).

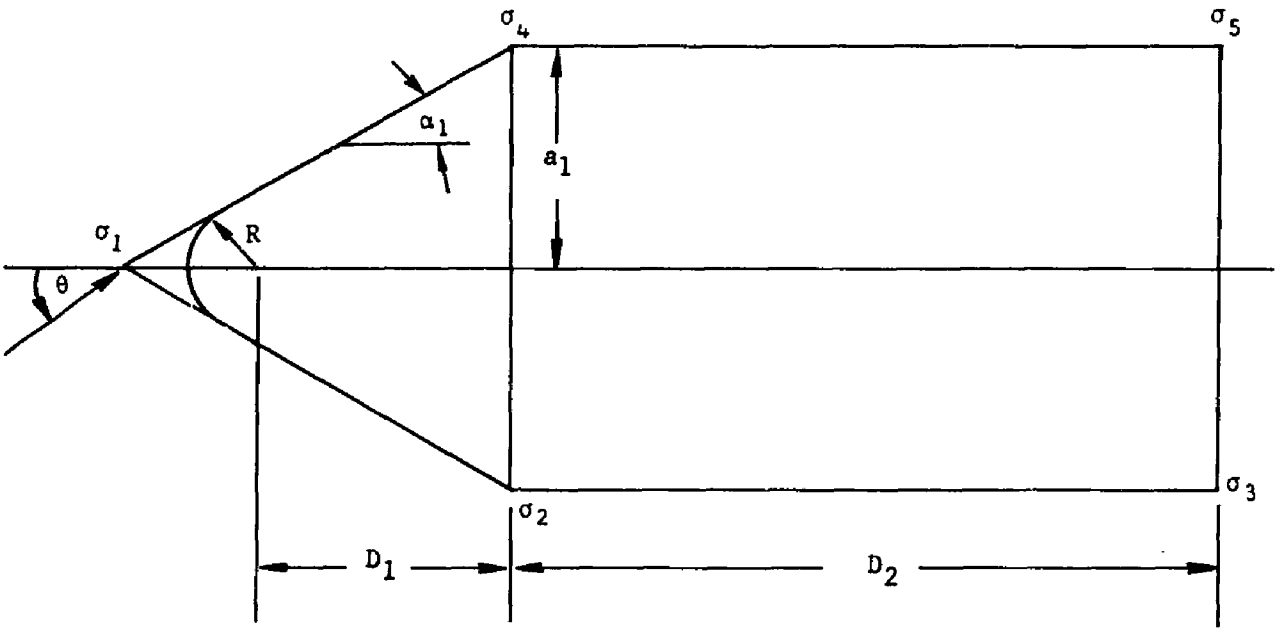

Figure G-1

The applicable equations are as follows:

$$\sigma_1 = \pi R^2 \text{ (If the nose is blunted)}$$

$$\sigma 2 = \frac{\lambda a_1}{8\pi} \frac{\tan^2 \alpha_1}{\sin \theta \cos^4 (1 - \tan \alpha_1 \tan \theta)^2}$$

for:

$$0 < |\theta| \leq \alpha_1$$

$$\alpha_1 \leq |\theta| < \frac{\pi}{2} - \alpha_1$$

$$\sigma_3 = \frac{\lambda a_1}{8\pi} \frac{\tan^2 (\alpha_1 - \theta)}{\sin \theta}$$

for:

$$0 < |\theta| \leq \alpha_1$$

$$\sigma_4 = \frac{\lambda a_1}{8\pi} \frac{\tan \theta}{\cos \theta}$$

for:

$$0 < |\theta| < \alpha_1$$

$$\alpha_1 < |\theta| < \frac{\pi}{2}$$

For normal incidence on the side of the front cone,

$$\sigma_{side_1} = \frac{8}{9} \frac{\pi a_1 3}{\lambda \cos \alpha_1 \sin^2 \alpha_1} \qquad \theta = \frac{\pi}{2} - \alpha_1$$

For nose-on incidence ($\theta = 0°$):

$$\sigma_{ring\ 2,4} = \pi a_1^2 \tan^2 \alpha_1$$

The geometrical distances of the cutting planes from the front reference plane (see text) are:

$$D_{12} = R + D_1 \cos \theta - a_1 \sin \theta$$

$$D_{13} = D_{12} + D_2 \cos \theta$$

$$D_{14} = D_{12} + 2a_1 \sin \theta$$

$$D_{15} = D_{13} + 2a_1 \sin \theta$$

APPENDIX H - CROSS SECTION OF BLUNTED CONE

The radar cross section equations pertaining to the cone configuration are given here. Figure H-1 shows the geometry for this case.

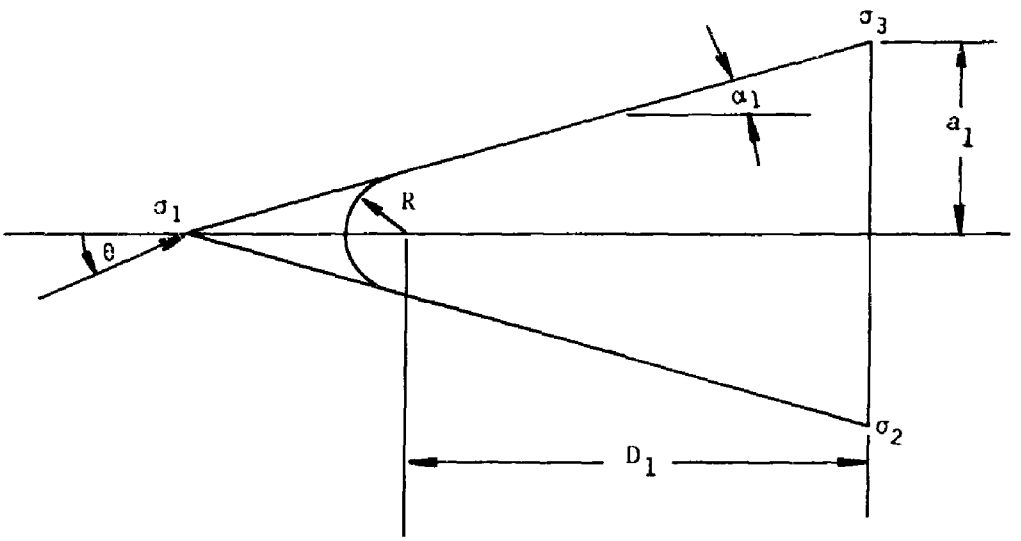

Figure H-1

The applicable equations are:

$$\sigma_1 = \pi R^2 \text{ (If the nose is blunted)}$$

$$\sigma_2 = \frac{\lambda a_1}{8\pi} \frac{\tan^2 (\theta + \alpha_1)}{\sin \theta}$$

for:

$$0 < \theta < \frac{\pi}{2} - \alpha_1$$

$$\frac{\pi}{2} - \alpha_1 < \theta < \frac{\pi}{2}$$

$$\sigma_3 = \frac{\lambda a_1}{8\pi} \frac{\tan^2 (\alpha_1 - \theta)}{\sin \theta}$$

For normal incidence on the side of the cone

$$\sigma_{side} = \frac{8}{9} \frac{\pi a_1^3}{\lambda \sin^2 \alpha_1 \cos \alpha_1}$$

for

$$|\theta| = \frac{\pi}{2} - \alpha_1$$

For nose-on incidence

$$\sigma = \pi a_1^2 \tan^2 \alpha_1 \qquad \theta = 0^o$$

The geometrical distances of the cutting planes from the front reference plane (see text) are:

$$D_{12} = R + D_1 \cos \theta - a_1 \sin \theta$$

$$D_{13} = D_{12} + 2a_1 \sin \theta$$

REFERENCES

1. Propagation of Short Radio Waves, Edited by Donald E. Kerr, Radiation Laboratory Series 13, pp. 445-481, 1951, Unclassified Report.

2. PLATO Air Defense System (U), Cornell Aeronautical Laboratory, 1 June 1954 to 31 December 1956, Secret Restricted Data Report.

3. Schensted, C. E., Crispin, J. W., and Siegel, K. M., Studies in Radar Cross Sections - XV - Radar Cross Sections of B-47 and B-52 Aircraft (U), University of Michigan, Engineering Research Institute, No. 2260-1-T, August 1954, Confidential Report.

APPROVED:

Stephen L. Johnston

STEPHEN L. JOHNSTON
Chief, Radiation Systems Branch

William C. McCorkle, Jr.

WILLIAM C. MCCORKLE, JR.
Director, Advanced Systems Laboratory

DISTRIBUTION

	Copy
U. S. Army Missile Command Distribution List A for Technical Reports (11 March 1963)	1-103
Massachusetts Institute of Technology Lincoln Laboratory P. O. Box 73 Lexington 73, Massachusetts	
Attn: Dr. P. C. Fritsch (B-268)	104,105
Dr. John Rheinstein (B-268)	106
Commanding General Electronics Research and Development Activity White Sands Missile Range, New Mexico	
Attn: Mr. Tom Bellows	107
Mr. Tom Reader	108
Cornell Aeronautical Laboratory, Inc. P. O. Box 235 Buffalo 21, New York	
Attn: Mr. Robert Wohlers	109
Mr. Robert Kell	110
Mr. Marley Bechtel	111
Radio Corporation of America Moorestown, New Jersey	
Attn: Mr. Eugene O'Donnell	112
Aerospace Corporation 2400 East El Segundo Boulevard El Segundo, California	
Attn: Mr. C. G. Bachman	113
AMCPM-ZE	114
-ZER, Mr. John Cremin	115
-SE	116
-MB	117
-PE	118
-HE	119
-HA	120
-MA	121
AMSMI-XS	122
-Y	123
-R	124
-RF	125
-RN	126
-RNT, Mr. Edward Dobbins	127
-RFD	128
-RFE, Mr. Max West	129-131
-RFS	132-156
-RB	157-161
-RAP	162